

In Situ IR Observation of Surface Species during the Photocatalytic Decomposition of Acetic Acid over TiO₂ Films

Shinri Sato,* Kazuhiro Ueda, Yasuhiro Kawasaki, and Ryuhei Nakamura

Catalysis Research Center and Graduate School of Environmental Earth Science, Hokkaido University, Sapporo 060-0008, Japan

Received: September 14, 2001; In Final Form: June 17, 2002

Surface-enhanced IR absorption spectroscopy (SEIRAS) was applied to in-situ observation of the adsorption states and the photocatalytic decomposition of acetic acid on Au/TiO₂ and Au/Pt/TiO₂ films. The adsorption states of acetic acid were determined in both the liquid and gas phase, and molecular adsorption was found to be dominant in the gas phase. Pt deposition on the TiO₂ film led to the formation of adsorbed methyl during the photodecomposition of gas-phase acetic acid, indicative of the formation of methyl radical as a reaction intermediate. The addition of gas-phase water to the system led to a significant increase in the coverage of adsorbed methyl as a result of enhancement in the reaction rate as reported before.

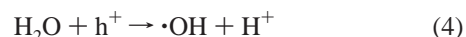
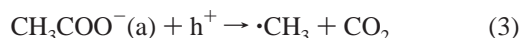
1. Introduction

In-situ observation of surface species during surface reactions such as heterogeneous catalytic processes is one of the important techniques to investigate a reaction mechanism. IR spectroscopy is probably the best method for this purpose among surface spectroscopies, because it is inexpensive, usable even at atmospheric pressure, and capable of determining chemical species.¹ The sensitivity of IR spectroscopy is, however, much lower than those of other surface vibrational spectroscopies such as HREELS, and in-situ observation during a reaction is virtually impossible in the presence of gas- or liquid-phase mediums that adsorb IR intensively.

Surface-enhanced IR absorption (SEIRA) has been observed for molecules adsorbed on an evaporated thin film of a free-electron metal such as Au or Ag and applied to surface analysis as SEIRA spectroscopy (SEIRAS).^{2–12} When SEIRAS is carried out in attenuated-total-reflection (ATR) configurations, it has a great advantage that IR measurements can be carried out even in an aqueous solution, because an IR beam hardly passes through the solution.^{6,9} Since the metal films used in SEIRAS are discontinuous and island-structure, SEIRAS can detect chemical species, which exist not only on the metal films but also in the vicinity of the metal islands, as evidenced previously.^{11,12} In the present study we applied SEIRAS to in-situ observation of surface species formed during the photocatalytic decomposition of acetic acid over bare and platinized TiO₂ film surfaces, on which an Au island film was deposited.

The photocatalytic decomposition of carboxylic acids over semiconductor surfaces is called photo-Kolbe reaction,¹³ and has been intensively studied as a typical photocatalytic reaction over platinized TiO₂ powders, which function as microphoto-electrochemical cells.¹⁴ The photo-Kolbe reaction of liquid-phase CH₃COOH was first investigated by Kreutler and Bard,¹³ who found that the reaction on bare as well as on platinized TiO₂ powders mainly gives CH₄ and CO₂ while the photoelectrochemical (PEC) reaction of CH₃COOH in a TiO₂–Pt PEC cell gives C₂H₆ at a TiO₂ photoanode and H₂ at a Pt cathode. They

explained this difference between a powdered system and a single-crystal system in terms of the following mechanism:¹³



For the reaction on powdered TiO₂, the density of $\cdot\text{CH}_3$ radicals is very low due to the large surface area of powdered TiO₂, and the sites for $\cdot\text{CH}_3$ production are very close to the sites for H(a) formation. As a result, the reaction of $\cdot\text{CH}_3$ radicals with H(a) (eq 8) occurs more favorably than the dimerization of $\cdot\text{CH}_3$ radicals (eq 6). For the reaction in a PEC cell, on the other hand, TiO₂ photoanode is a single crystal, specific surface area of which is very low, and H(a) is formed at a Pt counter electrode spatially separated from TiO₂ photoanode. As a result, the dimerization of $\cdot\text{CH}_3$ radicals dominates. We have also studied the photo-Kolbe reaction of gas-phase CH₃COOH over Pt/TiO₂ powders, and found the drastic enhancement of C₂H₆ formation upon the addition of gas-phase H₂O.^{15,16} This enhancement was ascribed to the acceleration of CH₃COOH decomposition by $\cdot\text{OH}$ radicals formed from H₂O (eq 5). The reaction on bare TiO₂ is very slow, giving CH₄ and CO₂, while the loading of Pt significantly promotes the reaction with a change in main products to H₂, CO₂, and C₂H₆.¹⁶ Au loading

* Corresponding author. Fax: +81-11-709-4748. E-mail: shinri@cat.hokudai.ac.jp.

instead of Pt loading, however, gives little effect on a reaction rate as well as on product distribution, since Au is quite inactive for hydrogen evolution.

Since radical formation was assumed for the photocatalytic reaction of CH_3COOH , ESR detection of radical species was attempted during the reaction, and $\cdot\text{CH}_3$ radical was detected using a spin trapping reagent.^{17,18} More recently, Kaise et al.¹⁹ employed a flow-cell ESR and directly observed $\cdot\text{CH}_3$ and $\cdot\text{CH}_2\text{COOH}$ radicals in aqueous metal/ TiO_2 suspensions at room temperature. Nosaka et al.²⁰ also detected $\cdot\text{CH}_3$ radical in the flow ESR measurements and assumed two reaction path ways for $\cdot\text{CH}_3$ radical formation from its dependence on a flow rate. Thus, $\cdot\text{CH}_3$ radical formation in the photocatalytic decomposition of CH_3COOH has been confirmed for aqueous Pt/ TiO_2 suspensions.

On the basis of the results obtained so far, the effects of Pt loading and $\text{H}_2\text{O}(\text{g})$ addition on the photocatalytic decomposition of CH_3COOH will be examined by SEIRAS.

2. Experimental Section

The details of sample preparation and experimental setup have been described in previous papers.^{11,12} Briefly, a transparent TiO_2 film coated on a CaF_2 disk (30 mm in diameter, 2 mm thick) by a standard sol-gel method was used as a photocatalyst. The disk was dipped into a TiO_2 sol prepared by the hydrolysis of Ti isopropoxide in 2-propanol, followed by drying in a N_2 atmosphere for 5 h and calcination in air at 500 °C for 3 h. TiO_2 films prepared by repeating this procedure three times exhibited pale blue color. Although the thickness of the films was not measured, it was estimated less than 500 nm from its transparency. Au and Pt deposition on the TiO_2 films was made by an evaporation method under a vacuum of 3×10^{-8} Torr. The thickness of metal films was monitored with a quartz film-thickness meter (Inficon XTM/2) and the deposition rate was controlled at 0.18 nm/min. The average thickness of the Au film was ca. 6 nm, while that of the Pt film ca. 1 nm.

For a gas-phase reaction, an evacuable IR cell was used, which was connected to a pumping and gas handling system. SEIRAS measurements were carried out in a backside reflection mode,^{11,12} in which an IR beam from FTIR (Horiba FT-300) was introduced from the CaF_2 side of the sample at the incident angle of ca. 50° and reflected at the interface between the TiO_2 and Au films. The reflected IR beam was collimated to an external MCT detector at liquid nitrogen temperature. This method enables us to observe surface species without the disturbance of IR absorption by gas- or liquid-phase reactants and products such as an ATR method. SEIRA spectra were recorded with the resolution of 4 cm^{-1} and with 200 scan. Acetic acid (99.5%) was used without further purification. Water and acetic acid were deaerated by repeating a freeze-and-thaw cycle for a gas-phase reaction. The vapor of water or acetic acid was introduced into the cell from a gas handling system equipped with a Baratron pressure gauge. A 1:1 mixture of gas-phase water and acetic acid was prepared by mixing their vapor at the same pressure in a glass reservoir. The light source was a high-pressure Hg lamp (Ushio UIV-570) that was filtered through a band-pass filter (Toshiba UV-D33S, 240–400 nm) and a water filter (10 cm long) to remove heat.

3. Results and Discussion

SEIRAS measurements were first applied to the adsorption of CH_3COOH in an aqueous solution, and the SEIRA spectra of CH_3COOH adsorbed on the Au/ TiO_2 film were successfully recorded as shown in Figure 1. In this measurement, liquid water

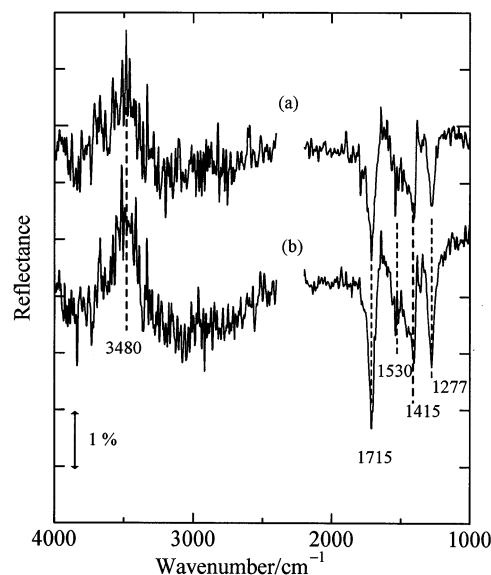


Figure 1. SEIRA spectra of CH_3COOH adsorbed on Au/ TiO_2 in an aqueous CH_3COOH solution. The spectrum of adsorbed water was subtracted. CH_3COOH concentration, (a) 8.3 vol %; (b) 16.6 vol %.

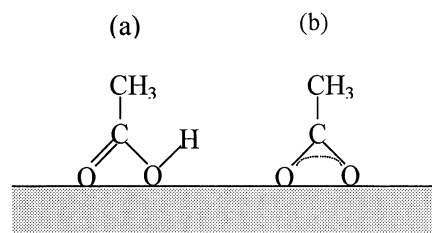


Figure 2. Adsorption states of (a) CH_3COOH and (b) CH_3COO^- on the sample.

was added first to the cell, followed by recording SEIRA spectrum as background, and then a calculated amount of $\text{CH}_3\text{COOH}(\text{l})$ was added to the cell. Therefore, the spectrum of adsorbed water is subtracted in Figure 1. The concentration of CH_3COOH is 8.3 vol % for spectrum (a) and 16.6 vol % for (b). An intense band at 1715 cm^{-1} is assigned to the $\text{C}=\text{O}$ stretching of carboxyl, while bands at 1530 and 1415 cm^{-1} are attributable to the antisymmetric and the symmetric stretching of $\text{O}-\text{C}-\text{O}$, respectively.²¹ The band at 1277 cm^{-1} is assigned to the stretching of $\text{C}-\text{O}$. A broad negative band around 3480 cm^{-1} is due to a decrease in the $\text{O}-\text{H}$ stretching band of adsorbed water, i.e., the removal of adsorbed water from the surface by CH_3COOH adsorption. The $\text{O}-\text{H}$ stretching of CH_3COOH is very broad and weak in its aqueous solution, since it is partly ionized. No bands due to $\text{C}-\text{H}$ stretching were observed. This is probably because the detection range of SEIRAS is so short (~ 1 nm) from a probe metal^{1,10} that the methyl groups of adsorbed CH_3COOH would not be detected when CH_3COOH adsorbs on the surface by COOH .

Since CH_3COOH exhibits the stretching bands of $\text{C}=\text{O}$, $\text{C}-\text{O}$, and $\text{O}-\text{H}$, while CH_3COO^- exhibits the antisymmetric and the symmetric stretching bands of $\text{O}-\text{C}-\text{O}$, these results indicate that both of them are adsorbed on the surface. Because SEIRAS is sensitive only to vibrational modes perpendicular to the surface (surface selection rule),¹ adsorbed CH_3COOH and CH_3COO^- would be oriented perpendicular to the surface as shown in Figure 2. One may suspect that the spectra observed here are the transmission spectra of CH_3COOH and CH_3COO^- , which enter into the bulk of TiO_2 film, since the film made by a sol-gel method is porous. If this were the case, then the Au

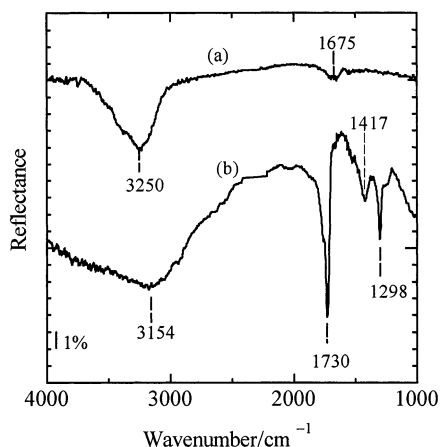


Figure 3. SEIRA spectra of (a) H_2O and (b) CH_3COOH adsorbed from gas phase onto Au/TiO_2 . H_2O pressure, 10 Torr; CH_3COOH pressure, 15 Torr.

film functions as a simple mirror. Au films are not necessarily SEIRA active, for example, when prepared under low vacuum conditions or deposited at a higher rate. The lack of SEIRA enhancement may be due to contaminations of the surface or the formation of continuous metal film. Such SEIRA inactive Au films give no spectrum in the presence of adsorbed species, even though it works as a mirror. This rules out the possibility that the SEIRA spectrum involves the transmission spectrum of species in the pores of the TiO_2 film. The TiO_2 films used are so thin that adsorbed species on the films could not be detected in an IR transmission mode.

Although TiO_2 films coated on a CaF_2 disk were stable in an aqueous CH_3COOH solution in the dark, the films were found to undergo dissolution to some extent under band gap illumination. Since SEIRAS is able to detect an atomic level change in surface composition, the photodissolution of TiO_2 films is a fatal problem. Since the films were found stable under illumination in the presence of gas-phase CH_3COOH , the gas-phase photo-reaction was investigated by SEIRAS to obtain reproducible results. Figure 3a shows the SEIRA spectrum of H_2O adsorbed at 10 Torr of $\text{H}_2\text{O}(\text{g})$, while Figure 3b shows the spectrum of CH_3COOH adsorbed from $\text{CH}_3\text{COOH}(\text{g})$ at 15 Torr. The spectral intensities of surface species adsorbed from gas phase were as good as those from liquid phase. All the spectra disappeared upon evacuating the cell, indicative of the physisorption of adsorbed species. The spectrum of CH_3COOH is very similar to those observed for $\text{CH}_3\text{COOH}(\text{l})$, but some differences are noticeable. The 1417 cm^{-1} band assigned to the symmetric stretching of $\text{O}-\text{C}-\text{O}$ is much lower in intensity than the 1730 cm^{-1} band assigned to the $\text{C}=\text{O}$ stretching, indicating that $\text{CH}_3\text{COO}^-(\text{a})$ is smaller in amount than $\text{CH}_3\text{COOH}(\text{a})$ as compared to the liquid-phase case. This may be due to the absence of $\text{H}_2\text{O}(\text{l})$, which could promote the ionization of CH_3COOH . The broad band centered at 3154 cm^{-1} is the OH stretching of CH_3COOH .

The Au/TiO_2 sample was exposed to a 1:1 mixture of $\text{CH}_3\text{COOH}(\text{g})$ and $\text{H}_2\text{O}(\text{g})$ at 15 Torr, and then irradiated to investigate a photoreaction mechanism. Difference SEIRA spectra between before and after UV irradiation are shown in Figure 4. The bands at 1734 , 1410 , and 1294 cm^{-1} decrease in intensity, and new bands appear at 3250 and 1592 cm^{-1} . Negative bands at 1734 , 1294 , and 1410 cm^{-1} indicate a decrease in the amounts of $\text{CH}_3\text{COOH}(\text{a})$ and $\text{CH}_3\text{COO}^-(\text{a})$. A weak band at 1592 cm^{-1} is attributed to surface carbonate species, which may be produced by the reaction of CH_3COO^- or CO_2 , which is a product of the reaction, with TiO_2 surface.

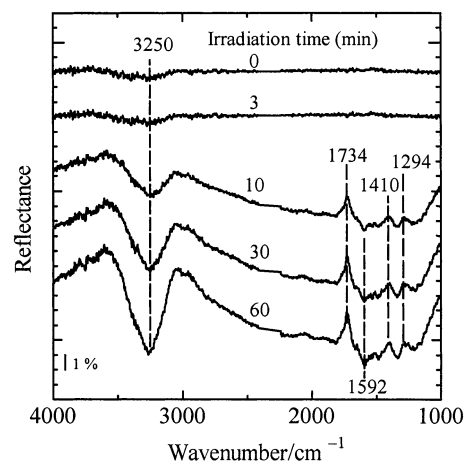


Figure 4. Difference spectra between before and after irradiation to Au/TiO_2 in the presence of a 1:1 mixture of $\text{CH}_3\text{COOH}(\text{g})$ and $\text{H}_2\text{O}(\text{g})$ at 15 Torr.

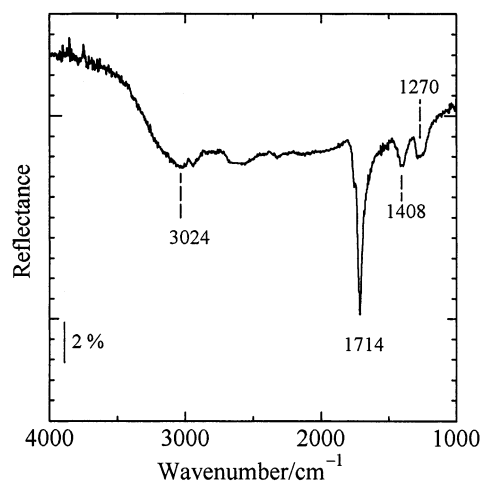


Figure 5. SEIRA spectrum of CH_3COOH adsorbed on Au/Pt/TiO_2 from $\text{CH}_3\text{COOH}(\text{g})$ at 15 Torr.

The decrease of $\text{CH}_3\text{COOH}(\text{a})$ and $\text{CH}_3\text{COO}^-(\text{a})$ may be due to the increase of reaction intermediates such as carbonates and photoadsorbed water, which compete for adsorption sites. An increased band at 3250 cm^{-1} is assigned to the $\text{O}-\text{H}$ stretching of adsorbed H_2O , which is produced by the oxidation of CH_3COOH . The photoenhanced adsorption of H_2O could occur as reported previously.¹² No other species were formed on the Au/TiO_2 film surfaces during the reaction.

To examine the effects of Pt loading on a reaction mechanism, the photodecomposition of $\text{CH}_3\text{COOH}(\text{g})$ over Au/Pt/TiO_2 film was investigated by SEIRAS. Figure 5 shows SEIRA spectrum of CH_3COOH adsorbed on Au/Pt/TiO_2 film from neat $\text{CH}_3\text{COOH}(\text{g})$ at 15 Torr, which is basically identical with that observed for the Au/TiO_2 . Therefore, Pt loading gives no effects on the adsorption states of CH_3COOH . Figure 6 shows difference spectra before and after UV irradiation in the presence of neat $\text{CH}_3\text{COOH}(\text{g})$ at 15 Torr. Negative bands at 1714 , 1412 , and 1296 cm^{-1} indicate the decrease of $\text{CH}_3\text{COOH}(\text{a})$ and $\text{CH}_3\text{COO}^-(\text{a})$ as already observed for the reaction on Au/TiO_2 . A broad band at 3274 cm^{-1} is assigned to the stretching of surface OH. The reason for this OH formation in the absence of $\text{H}_2\text{O}(\text{g})$ will be discussed later. Two weak bands at 2985 and 2878 cm^{-1} are assigned to the $\text{C}-\text{H}$ asymmetric and symmetric stretching of adsorbed CH_3 , respectively. The formation of $\text{CH}_3(\text{a})$ is a crucial difference between the reactions on Au/TiO_2 and on Au/Pt/TiO_2 , and would afford a clue to a

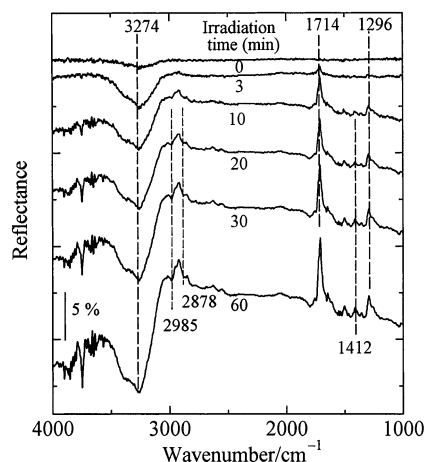


Figure 6. Difference spectra between before and after irradiation to Au/Pt/TiO₂ in the presence of neat CH₃COOH(g) at 15 Torr.

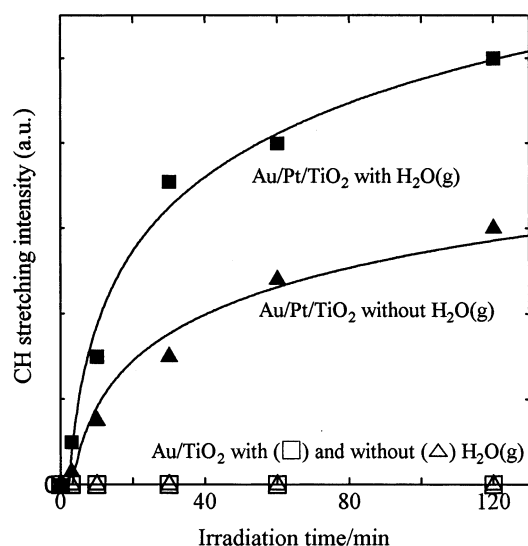


Figure 7. Time dependence of the band intensities of C–H stretching during the photocatalytic decomposition of CH₃COOH(g) on Au/TiO₂ and Au/Pt/TiO₂ in the presence and absence of H₂O(g).

mechanism of the reaction. A sharp band at 3750 cm⁻¹ was not reproducible and would be due to a systematic error of the spectroscopy, since a dynamic range of our FTIR machine is too narrow to accumulate accurately low-intensity signals in this region. We have found that the addition of H₂O(g) drastically enhances the photocatalytic reaction of CH₃COOH(g) on Pt/TiO₂.^{15,16} To examine the effects of H₂O(g), SEIRAS measurements were carried out for the photocatalytic reaction of a 1:1 mixture CH₃COOH(g) and H₂O(g). Spectral features were virtually identical with those observed for the reaction of neat CH₃COOH(g), but the bands attributed to CH₃(a) grew up at a higher rate than in the absence of H₂O(g) as shown in Figure 7. This result would be resulted from acceleration of the reaction by the addition of H₂O(g) as reported before.

The present SEIRAS measurements show that CH₃(a) is formed during the photodecomposition of CH₃COOH(g) on Au/Pt/TiO₂ but not on Au/TiO₂. The formation of CH₃(a) could arise from the adsorption of •CH₃ radicals on the surface, and the coverage of CH₃(a) may depend on the rate of •CH₃ radical formation. For the reaction of CH₃COOH(g), •CH₃ radicals would not be stabilized by hydration unlike in aqueous solutions so that they would be spontaneously adsorbed on the surface.

The photodecomposition of CH₃COOH on bare TiO₂ is known to be much slower than that on Pt/TiO₂.^{13,16} The absence of CH₃(a) in the reaction on Au/TiO₂ is basically due to the slow decomposition of CH₃COOH. On the other hand, the addition of H₂O(g) enhances the photodecomposition of CH₃COOH(g) on Pt/TiO₂ as mentioned above, and as a result, the coverage of CH₃(a) increases, as shown in Figure 7, due to an increase in the concentration of •CH₃ radicals. One may suppose here that the reaction of •CH₃ radicals with H(a) (eq 8) would be also enhanced by the addition of H₂O(g), since H(a) production is also enhanced. The formation of CH₄ is, however, less enhanced by the addition of H₂O(g) to the photodecomposition of CH₃COOH(g) over Pt/TiO₂ than the formation of C₂H₆.^{15,16} This arises from its reaction mechanism, in which H(a) is produced on Pt sites, while •CH₃ radical formation occurs on TiO₂ sites.^{13,14} Therefore, CH₄ formation requires the migration of •CH₃ radicals from TiO₂ sites to Pt sites or the spillover of H(a) from Pt sites to TiO₂ sites.

A question in the present SEIRAS measurements is a significant increase in O–H stretching band during the photodecomposition of neat CH₃COOH(g) on Au/Pt/TiO₂ (Figure 6). One of the reasons for this O–H band increase is transformation of H₂O(a), which remains after room-temperature pumping, toward a strongly adsorbed one under irradiation as reported previously.¹² This transformation is accompanied by OH band shift to lower frequencies.¹² Another factor is the adsorption of impurity H₂O (0.5%) in acetic acid. These factors are, however, too small to explain the large increase of OH band, since the amount of H₂O(a) remained after pumping as well as impurity H₂O in CH₃COOH is very small. There should be, therefore, other factors to increase the O–H band. Although all H(a) atoms are thought to desorb as H₂ in eq 9, some H(a) atoms may spillover from Pt to TiO₂ surfaces and hydrogenate TiO₂ to produce surface hydroxyls. In addition a TiO₂ film prepared by a sol–gel method undergoes photodissolution under acidic conditions, which may also produce surface hydroxyls.

In summary, in-situ SEIRAS can determine the adsorption states of CH₃COOH on TiO₂ films and detect reaction intermediates such as CH₃(a) during the photocatalytic decomposition of CH₃COOH. These observations could not be performed by conventional IR spectroscopy. Thus, SEIRAS is a promising spectroscopy to observe submonolayer quantities of surface species in the presence of reactants and to investigate a mechanism of catalytic processes.

References and Notes

- (1) Suétaka, W. *Surface Infrared and Raman Spectroscopy*; Plenum Press: New York, 1996.
- (2) Hartstein, A.; Kirtly, J. R.; Tsang, C. T. *Phys. Rev. Lett.* **1980**, *45*, 201.
- (3) Hatta, A.; Suzuki, Y.; Suétaka, W. *Appl. Phys.* **1984**, *A35*, 135.
- (4) Kamata, T.; Kato, Umemura, J.; Takenaka, T. *Langmuir* **1987**, *3*, 1150.
- (5) Osawa, M.; Ikeda, M. *J. Phys. Chem.* **1991**, *95*, 9914.
- (6) Osawa, M.; Ataka, K.; Yoshii, K.; Yotsuyanagi, T. *J. Electron Spectrosc. Relat. Phenom.* **1993**, *64/65*, 371.
- (7) Osawa, M.; Ataka, K.; Yoshii, K.; Nishikawa, Y. *Appl. Spectrosc.* **1993**, *47*, 1497.
- (8) Nishikawa, Y.; Fujiwara, K.; Ataka, K.; Osawa, M. *Anal. Chem.* **1993**, *65*, 556.
- (9) Ataka, K.; Yotsuyanagi, T.; Osawa, M. *J. Phys. Chem.* **1996**, *100*, 10664.
- (10) Sato, S.; Suzuki, T. *Appl. Spectrosc.* **1997**, *51*, 1170.
- (11) Sato, S.; Kamada, K.; Osawa, M. *Chem. Lett.* **1999**, 15.
- (12) Nakamura, R.; Ueda, K.; Sato, S. *Langmuir* **2001**, *17*, 2298.
- (13) Kreutler, B.; Bard, J. A. *J. Am. Chem. Soc.* **1978**, *100*, 2239, 5985.
- (14) Bard, A. J. *J. Photochem.* **1979**, *10*, 59. *Science* **1980**, *207*, 139. *J. Phys. Chem.* **1982**, *86*, 172.

- (15) Sato, S. *J. Chem. Soc. Chem. Commun.* **1982**, 26.
- (16) Sato, S. *J. Phys. Chem.* **1983**, 87, 3531.
- (17) Jaeger, C. D.; Bard, A. J. *J. Phys. Chem.* **1979**, 83, 3146.
- (18) Kraeutler, B.; Jaeger, C. D.; Bard, A. J. *J. Am. Chem. Soc.* **1978**, 100, 4903.
- (19) Kaise, M.; Kondoh, H.; Nishihara, C.; Nozoe, H.; Shindo, H.; Nimura, S.; Kikuchi, O. *J. Chem. Soc. Chem. Commun.* **1993**, 395. Kaise, M.; Nagai, H.; Tokuhashi, K.; Kondo, S.; Nimura, S.; Kikuchi, O. *Langmuir* **1994**, 10, 1345.
- (20) Nosaka, Y.; Koenuma, K.; Ushida, K.; Kira, A. *Langmuir* **1996**, 12, 736. Nosaka, Y.; Kishimoto, M.; Nishino, J. *J. Phys. Chem. B* **1998**, 102, 10279.
- (21) Fifield, F. W.; Kealey, D. *Principles and Practice of Analytical Chemistry*, Japanese Edition; Maruzen: Tokyo, 1998.